International Journal of Engineering Trends and Technology
ISSN: 2231 – 5381 /doi:10.14445/22315381/IJETT-V70I2P2236

Volume 70 Issue 2, 305-310, February, 2022

Original Article

Comparative Analysis and Switching Requirements of 1Ø Grid Connected Non-Isolated Inverters

Rushikesh S.Shahakar[1], Kawita D. Thakur[2]

[1]*Research Scholar, Department of Electrical Engineering, Government College of Engineering, Amravati, India.*
[2]*Assistant Professor, Department of Electrical Engineering, Government College of Engineering, Amravati, India*

[1]rsshahakar@gmail.com, [2]kawitadthakur@gmail.com

Abstract *— Recent surveys reveal that impact of the electrical grid on specific global demands of energy is expected to climb 25% by 2040. It is a great hike, and the whole world is expected to increase its per capita income in a green and clean manner. To meet this requirement by using renewable generation, power electronics devices play a crucial role. The efficiency of the generation system greatly relies on converter topologies.*

The paper focus on 1Ø grid linked inverter topologies that are not isolated. A comparison of four single-phase topologies is shown, including full bridge, H_5, H_6 and HERIC inverters. A discussion of topologies is carried out on the basis of common-mode voltage stability, leakage current, needs of the gate driver circuit, conduction loss and efficiency. The analysis presented assists to select appropriate inverter topology for a specific application in a PV system.

Keywords *— Non-isolated inverters, Switching requirements, Common mode voltage, PV system.*

I. INTRODUCTION

India has to contribute about 45% of world energy demand growth up to 2040. In this photovoltaic (PV) energy have to contribute significantly, as it is a free and clean source of energy along with a variety of application [1]. At present, only 33730.56 MW of energy is generated in India by using PV generation [2]. Micro-grid is also gaining importance because of ancillary services provided by distributed energy resources and reduced transmission losses [3-7]. To increase generation by penetrating renewable energy sources into micro-grid and utilization of that power in distribution network without adverse effects on protection, a robust power conditioning unit is required [8,9].

The number of stages engaged in the power conditioning unit is the primary challenge in achieving higher efficiency when supplying electricity to the grid in a single-phase grid linked system[10,11]. Single-stage conversion system omits low-frequency transformer as shown in fig. 1(b). Double stage conversion system presented in fig. 1(a) not only enormously reduces the efficiency of the system but also make the system bulky and costly. On the other hand, single-stage conversion has the drawback of not feeding power when PV voltage undershot the grid voltage's peak value.

In single-stage conversion, inverter topology plays a major role. The paper introduces an overview of the single-stage conversion system of non-isolated string inverters [12 – 16]. The following are the sections of the paper: The second section is about operating modes of inverter topologies and their mathematical expression for common-mode voltage. The third section justifies the requirements of switching and different ways of providing them. It also comments on factors affecting the gate driver circuit and its solution. Section four relates to comparative analysis of topologies based on various parameters, and conclusions will be drawn in section five.

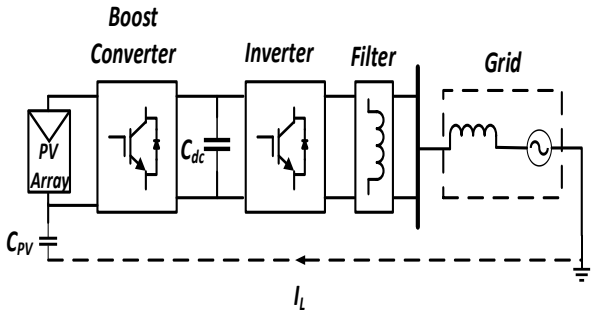

Fig.1(a) Double stage conversion

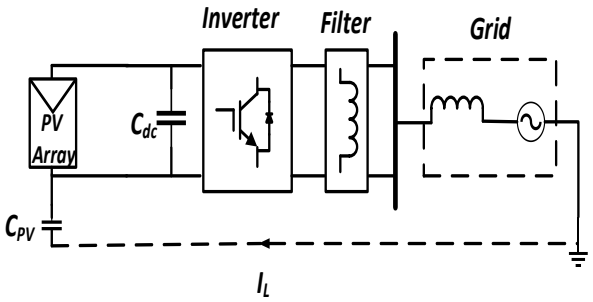

Fig.1(b) Single-stage conversion

II. INVERTER TOPOLOGIES

There are several transformerless topologies of inverters depending on their output levels, input and place of implementation [12, 17, 18]. The current source inverter is

not preferred as it introduces a very high ground leakage current [19]. The literature in this section focuses on working on four single-phase three-level voltage source topologies, namely H-bridge, H_5, H_6 and HERIC and their common-mode voltage. The working of topologies is divided into four operating modes, i.e. active conduction state (Mode-1) and freewheeling mode (Mode-2) for a positive half period, whereas Mode-3 is active conduction state and Mode- 4 is a negative half period freewheeling mode.

A. Operating Modes of Topologies

a) H- bridge

The half-bridge inverter is a simple conversion architecture used in PV applications. However, the requirement of DC link voltage is much higher, and switches must be able to endure this high dc-link voltage stress [20]. As a result, the full-bridge inverter (fig. 2.1) became commercially available. Grid frequency is used to run the top switches, whereas switching frequency is used by the bottom switches. Table 1 lists the operating modes of the H bridge inverter in detail.

All of the other topologies mentioned further in this section can be achieved by providing a bypass path, as shown in fig. 2.2 at DC or AC side. Bypassing helps not only grid and PV isolation but also avoids reactive power exchange during the freewheeling mode. As a result, the inverter's efficiency can be improved.

b) H_5 Topology

The H5 topology is produced by connecting the positive of the DC side to the H-bridge at DC bypass 1 with an additional switch (S5), as seen in fig. 2.3.

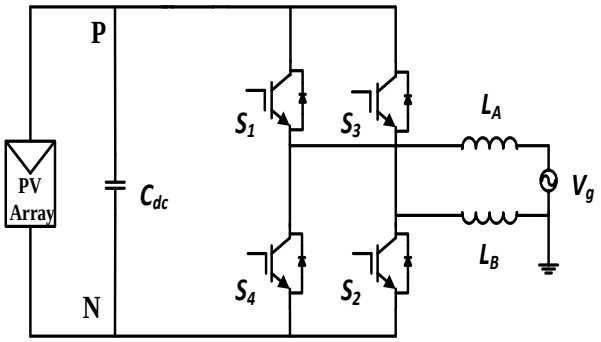

Fig.2.1 Full bridge inverter

Table1. Operating Modes of Full-Bridge Topology

Sr. No.	Switch State (ON/OFF)	Output Voltage (V_{ab})	Mode of Operation
1	i) S_1, S_2 - ON ii) S_3, S_4 - OFF	$+V_{dc}$	Mode-I
2	i) S_1, D_3 - ON ii) S_2, S_3, S_4 - OFF	0	Mode-II
3	i) S_3, S_4 - ON ii) S_1, S_2 - OFF	$-V_{dc}$	Mode-III
4	i) S_3, D_1 - ON ii) S_4, S_1, S_2 - OFF	0	Mode-IV

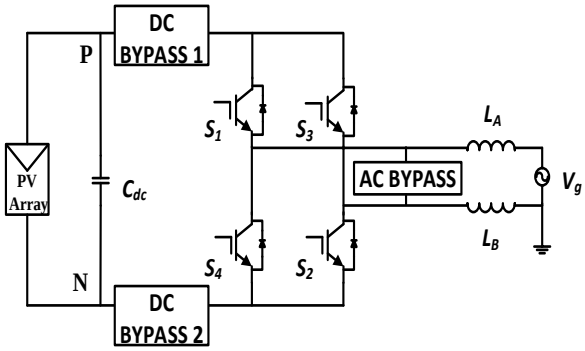

Fig. 2.2 H-bridge with Bypass

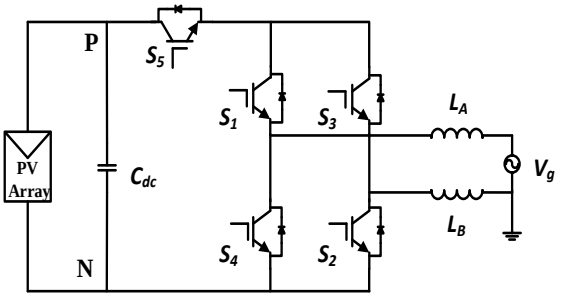

Fig. 2.3. H_5 Topology of Inverter

This additional switch is operated in synchronization with the lower switches and provide DC bypass. This helps to decouple H-bridge from the PV array during modes II and IV. Upper switches and lower switches are operated similarly to that of H-bridge. The state of switches in accordance with the different operating modes is shown in table 2.

c) HERIC Topology

As seen in fig. 2.4 includes two more switches (S5 & S6) on the grid side, as well as an H-bridge. During each half cycle, a group of diagonal switches in the H-bridge operate at a switching frequency. Two switches in bypass run at grid frequency, each conducting for half of the grid voltage cycle. During modes II and IV, the AC side can be short-circuited to achieve zero voltage using these additional switches and associated antiparallel diodes, as indicated in Table 3.

Table 2. Operating Modes of H_5 Topology

Sr. No.	Switch State (ON/OFF)	Output Voltage (V_{ab})	Mode of Operation
1	i) S_1, S_2, S_5 - ON ii) S_3, S_4 - OFF	$+V_{dc}$	Mode-I
2	i) S_1, D_3 - ON ii) S_2, S_5, S_3, S_4 -OFF	0	Mode-II
3	i) S_3, S_4, S_5 - ON ii) S_1, S_2 - OFF	$-V_{dc}$	Mode-III
4	i) S_3, D_1 - ON ii) S_4, S_5, S_1, S_2 -OFF	0	Mode-IV

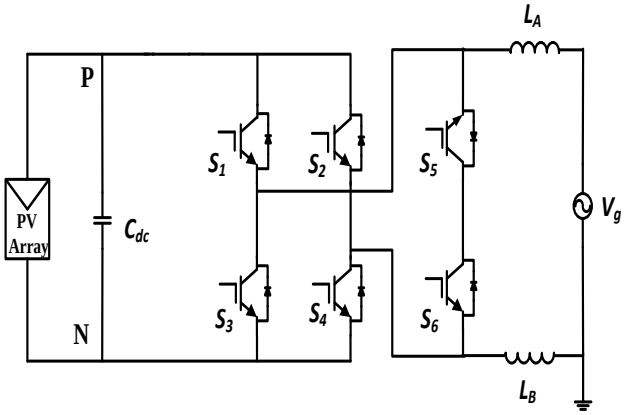

Fig. 2.4 HERIC topology of inverter

Table 3. Operating Mode of HERIC Topology

Sr. No.	Switch State (ON/OFF)	Output Voltage (V_{ab})	Mode of Operation
1	i) S_1, S_2, S_5 - ON ii) S_3, S_4, S_6 - OFF	$+V_{dc}$	Mode-I
2	i) S_5, D_6 - ON ii) S_1, S_2, S_3, S_4, S_6 - OFF	0	Mode-II
3	i) S_3, S_4, S_6 - ON ii) S_1, S_2, S_5 - OFF	$-V_{dc}$	Mode-III
4	i) S_6, D_5 - ON ii) S_1, S_2, S_3, S_4, S_5 - OFF	0	Mode-IV

d) H_6 Topology:

The H6 topology circuit depicted in fig. 2.5 is made up of four switches (S1-S4) forming an H-bridge. Additional two secondary switches along with two diodes are also used. Diodes help to create a clamping branch, and the freewheeling channel is clamped to half the input voltage with the use of a capacitor divider.

As stated in table 4, H-bridge switches are triggered at grid frequency, whereas secondary switches are triggered at switching frequency. Secondary switches offer DC bypass, and the DC bypass switches S5 and S6 are turned off to obtain zero output voltage.

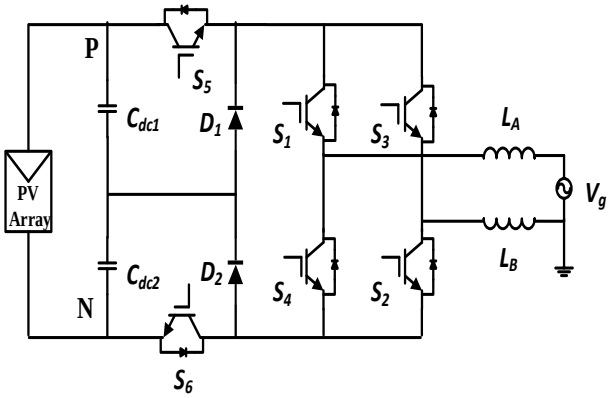

Fig. 2.5. H_6 topology of inverter

Table 4. Operating Modes of H_6 Topology

Sr. No.	Switch State (ON/OFF)	Output Voltage (V_{ab})	Mode of Operation
1	i) S_1, S_2, S_5, S_6 - ON ii) S_3, S_4 - OFF	$+V_{dc}$	Mode-I
2	i) S_1, S_2 - ON ii)S_5, S_6, S_3, S_4-OFF	0	Mode-II
3	i) S_3, S_4, S_5, S_6 - ON ii) S_1, S_2 - OFF	$-V_{dc}$	Mode-III
4	i) S_3, S_4 - ON ii) S_5, S_6, S_1, S_2 - OFF	0	Mode-IV

B. Common Mode Voltage and Leakage Current

The absence of a transformer (galvanic isolation) in a single-stage conversion system, leakage current forms a closed path between PV array and grid is depicted in fig.1. (b). Relying on the generation mechanism of leakage current, transformerless inverters may be divided into two groups: asymmetrical and symmetrical inductor-based groups [20,21]. The mean value of voltages between the inverter's outputs and a common reference causes leakage current. This leakage current endangers workers' safety, creates electromagnetic interference, increases losses, and causes current ripples [22]. As a result, DIN VDE 0126-1-1 is a German standard that must be followed for safety reasons. PV must be detached before 0.3 seconds if the value of leakage current surpasses the RMS value of 300 mA [23].

Isolation can be provided in transformerless inverter by using DC or AC bypass, as shown in fig 2.2. H_5 and H_6 employ DC bypass, but the extra switch is introduced in the conduction path; hence conduction losses increase. On counter side employment of AC bypass in HERIC exclude conduction of extra switches and perform freewheeling. Therefore as compared to DC bypass topologies, using AC bypass has lower conduction loss. Despite this, due to the impact of stray capacitances and parasitic elements, bypass for galvanic isolation is unable to totally eliminate leakage current. As demonstrated in fig. 2.6, a transformerless inverter creates a resonant circuit.

$$V_{CM} = \frac{V_{AN} + V_{BN}}{2} \quad (1)$$

$$V_{DM} = V_{AN} - V_{BN} \quad (2)$$

The output voltage can be calculated using (1) and (2)

$$V_{AN} = V_{CM} + \frac{V_{DM}}{2} \quad (3)$$

$$V_{BN} = V_{CM} - \frac{V_{DM}}{2} \quad (4)$$

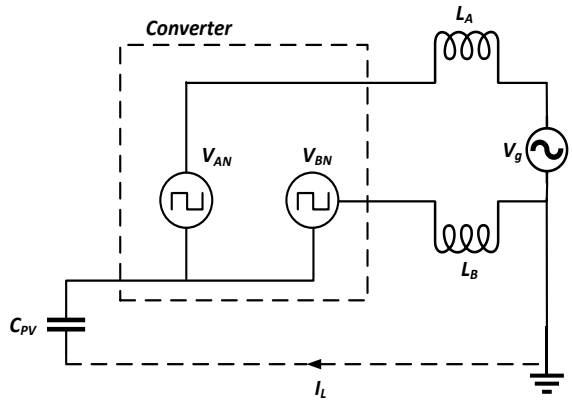

Fig.2.6 Resonant circuit of PV system

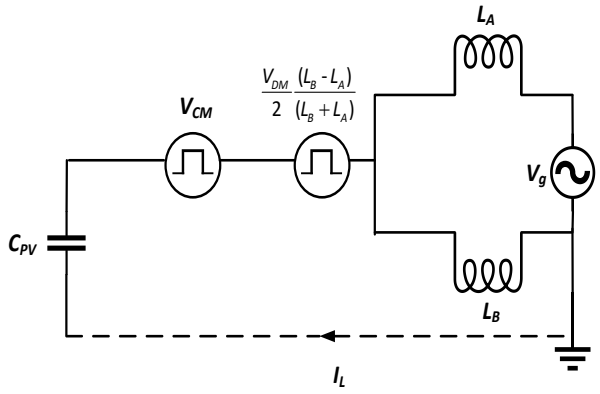

Fig.2.7 PV system with common-mode model

As seen in equations (3), (4), and fig. 2.7, common-mode voltage affects leakage current. To eliminate leakage current by creating common-mode voltage, the inverter architecture and modulation mechanism must be properly established. Because the V_{AN} and V_{BN} under each operating mode are distinct, the model illustrated in fig. 2.7 is valid for analyzing the other topologies provided here. The two rules [24] can be used to remove leakage current in full-bridge and half-bridge inverters. Rule 2 does not apply to full bridge symmetrical topologies; hence a clamping branch must be introduced as per rule 1. A common mode conduction route into the inverter system is the second technique to eliminate leakage current [25]. As a result of the lack of additional active components, system complexity and cost can be decreased. During freewheeling mode in H5 and HERIC, the dc-link is isolated from the grid. Because the voltage at points A and B is floating in relation to the DC connection, oscillations in the common-mode voltage cause leakage current. Galvanic isolation isn't enough to totally eliminate the leakage current. Common mode voltage clamping, as utilized in H6, combined with galvanic isolation via bypass, is a solution for totally eliminating leakage current.

III. SWITCHING TECHNIQUES & REQUIREMENTS

Sinusoidal pulse width modulation is the most common method of switching semiconductor devices (SPWM). The primary goal of SPWM is to manage the AC side voltage while also reducing harmonic voltages and their detrimental effects. The SPWM can be used in a variety of industries, including renewable energy systems, machine drives, and so on. They are divided into three categories: bipolar (BPWM), unipolar (UPWM), and hybrid (HPWM). In contrast to bipolar and unipolar techniques, in an H-bridge, two of the switches are high frequency, while the other two are low frequency [26]. This results in a smoother output voltage than bipolar, as well as lower switching losses. HPWM's switching loss is similar to UPWM's, and it's around half that of BPWM [27]. To achieve the same total harmonic distortion (THD), bipolar PWM switches at 3.6 times the frequency of unipolar or hybrid PWM [28]. Table 5 highlights the various elements of BPWM and HPWM. It can be stated that the hybrid PWM technique is superior in every way except the control scheme design.

Improper modulation schemes have a direct impact on system efficiency and size. Similarly, using a high number of power supplies for switching puts the system's size at risk. To reduce it, if a single power source is used to operate switches on the same leg, the switches would short circuit, which is undesirable. The source terminals of high-side switches, on the other hand, are not directly linked to the ground, making gate driving more difficult. A pulse transformer can be used to create isolation as well as operate the inverter's high side switch. However, using a transformer not only makes the circuit more complicated but also makes the system bigger. Low-side switches are easily actuated since their source terminals are connected to ground potential. As a result, the power supply required for driving gates changes depending on the architecture of the inverter topology, as indicated in Table VI.

Individual power supplies required for H-bridge and HERIC topology are the same and lowest. On the other hand, five supplies are required for H_6 topology, which is the highest. The use of isolated supply make the system costly as well as bulky, and to overcome this issue, bootstrap is the best solution. The bootstrap circuit includes capacitors, resistors and diodes, which are light in weight as well as cheaper [29]. By using a single power supply and bootstrap, it is possible to drive high side switches. Building three floating supplies by using bootstrap, HERIC topology can be driven only by using a single power supply [30].

IV. COMPARISION

Examining the architecture and operating modes of H-bridge, H_5, HERIC and H_6 in section I total a number of switches, as well as switches in the conductive path, can be found out. HERIC & H_6 require six semiconductor switches, which increase the cost and weight of the system. In the course of active voltage state, out of all topologies discussed in the paper, H_6 has the highest conducting switches. H_6 topology has four switches in conduction, which results in higher conduction loss.

Table 5. Comparison of Bipolar & Hybrid PWM

Sr. No.	Parameter	Bipolar PWM	Hybrid PWM
1	Voltage levels in output	2	3
2	Harmonic content in output	High	Low
3	Size of filter	Big	Small
4	Cost of filter	High	Less
5	Switching losses	More	Less
6	Design of control	Easy	Complex
7	Power quality	Low	High

Table 6. Requirement of Power Supply

Sr. No.	Inverter Topology	Isolated Supply Required
1	H-bridge	3
2	H_5	4
3	HERIC	3
4	H_6	5

H_5, HERIC and H_6 topologies are commercialized by different industries. A product containing these topologies having an AC output power of 5 kW is compared here. H_5 is commercialized by SMA (Sunny-Boy 3000 - 5000 TL). Maximum efficiency of 97 % and a European efficiency of 96.5 % is reported for 5 kW output power [31]. The HERIC topology is used by Sunways in the AT series. According to the manufacturer, the highest efficiency of this product is 95.5 percent, with a European efficiency of 95 percent [32]. The commercialized H_6 inverter presented by INGECON (SUN I Play TL M Series) gives the highest efficiency of 98 percent with a European efficiency of 97.6 percent [33]. H_6 has the highest efficiency as the voltage of secondary switches is limited to half of the DC-link voltage. Compared to HERIC, H_5 has higher efficiency, as shown in Table VII. H_5 contains only one switch which operates at high frequency. On the other hand, HERIC has two.

V. CONCLUSION

The paper provides a thorough investigation of single-phase transformerless inverters for photovoltaic applications. The topologies of H-bridge, H_5, H_6 and HERIC topologies are evaluated based on parameters like number of switches used, switch in conduction path, conduction loss, number of individual power supply required, leakage current, efficiency and common-mode voltage. The use of individual power supply makes the system bulky and costly. H_6 topology requires the highest individual supply for gate driver compared to H_5, HERIC and H-bridge. To reduce the weight of the system by utilizing a minimum power supply and making it economical, one bootstrap circuit is the perfect solution. The modulation scheme affects the power quality, size and cost of the system. Hybrid modulation is found better in every aspect, excluding the complexity of the design.

The current of leakage is determined by the common-mode voltage, and according to DIN VDE 0126-1-1, it must be below the RMS value of 300 mA. The aim of the complete elimination of leakage current can be achieved successfully by providing both bypass and common-mode voltage clamping. H_6 topology satisfies these conditions, and hence leakage current is minimum. Therefore commercialized inverter having H_6 architecture has a maximum efficiency of 97.6% related to H_5, HERIC and H-bridge. Considering all factors in the literature, the H_6 topology was found out to be a promising one.

Table 7. Comparison of Inverter Topologies

Sr No	Parameter	H bridge	H_5	HERIC	H_6
1	Total device used	4	5	6	6
2	Device in conduction	2	3	3	4
3	Conduction loss	low	moderate	moderate	high
4	Common mode voltage	constant	floating	floating	constant
5	Maximum efficiency	78.46%	97.0%	95.5%	98%
6	European efficiency	78.27%	*96.5%*	*95.0%*	97.6%

REFERENCES

[1] Dr Chetansingh Solanki, .,Solar Photovoltaic's Fundamentals Technologies and Application" 2nd edition, (2011).

[2] State-wise installed capacity of grid Interactive Renewable power as on 31-12-2019 (Posted on 09.01.2020)- MNRE Report https://mnre.gov.in/ physical-progress-achievements, accessed: (2020) 01-10

[3] Xuan Liu, Bin Su ., Microgrids - An Integration of Renewable Energy Technologies, Technical Session 3 Protection, Control, Communication and Automation of Distribution Network, CICED 2008

[4] Zhenhua Jiang and Xunwei Yu, Hybrid DC- and AC-Linked Microgrids: Towards Integration of Distributed Energy Resources, IEEE Energy 2030, Atlanta, GA USA, (2008) 17-18.

[5] G. Adinolfi, V. Cigolotti, G. Graditi and G. Ferruzzi, Grid integration of Distributed Energy Resources: Technologies, potentials contributions and future prospects, IEEE (2013).

[6] Xiaoyan Yu, Leon M. Tolbert, Ancillary Services Provided from DER with Power Electronics Interface, IEEE ., (2006).

[7] Benjamin Kroposki, Christopher Pink, Richard DeBlasio, Holly Thomas, Marcelo Simoes and Pankaj K. Sen, Benefits of Power Electronic Interfaces for Distributed Energy Systems, IEEE Transaction on Energy Conversion, 25(3) (2010) 901- 908.

[8] Gurkiran Kaur, Mohammad Vaziri Y., Effects of Distributed Generation (DG) Interconnections on Protection of Distribution Feeders, IEEE (2006).

[9] J.Driesen and R.Belmans, "Distributed Generation: Challenges and Possible Solutions, IEEE, (2006).

[10] Yaosuo Xue, Liuchen Chang, Soren Baekhoj Kjaer, Josep Bordonau and Toshihisa Shimizu, Topologies of Single-Phase Inverters for Small Distributed Power Generators: An Overview, IEEE Transaction on Power Electronics, 19(5) (2004).

[11] Dipankar Debnath and Kishore Chatterjee, A Buck-Boost Integrated Full Bridge Inverter for Solar Photovoltaic Based Standalone System, IEEE , (2013).
[12] S. B. Kjaer, J. K. Pedersen, and F. Blaabjerg, A Review of Single-Phase Grid-Connected Inverters for Photovoltaic Modules, IEEE Trans. On Ind. Appl., 41(5) (2005) 92–1306.
[13] Jinia Roy, Yinglai Xiay and Raja Ayyanar, Performance Evaluation of Single-Phase Transformer-less PV Inverter Topologies, IEEE, (2018).
[14] M. Victor, F. Greizer, S. Bremicker, and U. Hübler, Method of Converting A Direct Current Voltage from A Source of Direct Current Voltage, More Specifically from A Photovoltaic Source of Direct Current Voltage, Into an Alternating Current Voltage, US Patent US7 411 802 B2, August 12 (2008).
[15] H. Schmidt, C. Siedle, and J. Ketterer, DC/AC Converter to Convert Direct Electric Voltage into Alternating Voltage or Into Alternating Current," US Patent US7 046 534 B2, 16 (2006).
[16] R. Gonzalez, J.Coloma, J. Lopez, and L. Marroyo., Single-Phase Inverter Circuit To Condition And Transform Direct Current Electric Power Into Alternating Current Electric Power., US Patent US 2009/0 316 458 A1, 24 (2009).
[17] O. Lopez, R. Teodorescu, and J. Doval-Gandoy, Multilevel Transformerless Topologies for Single-Phase Grid-Connected Converters, in IEEE Ind. Electron., IECON 2006 - 32nd Annual Conference, (2006) 5191–5196.
[18] M. Calais and V. G. Agelidis, Multilevel Converters For Single-Phase Grid-Connected Photovoltaic Systems-An Overview, in Ind. Electron., 1998. Proceedings. ISIE '98. IEEE Int. Symposium on, 1 (1998) 224–229.
[19] S. Anand, S. K. Gundlapalli, and B. G. Fernandes, Transformer-Less Grid Feeding Current Source Inverter for Solar Photovoltaic System, IEEE Trans. on Ind. Electron., 61(10) (2014) 5334–5344.
[20] Wuhua Li, E, Yunjie Gu, Haoze Luo, Wenfeng Cui, Xiangning He and Changliang Xia, Topology Review and Derivation Methodology of Single-Phase Transformerless Photovoltaic Inverters for Leakage Current Suppression, IEEE Transaction on Industrial Electronics, 10, (2015).
[21] R.Antony Raja Sekar, D.Arun Prasad, Improved Transformer-less Inverter for PV Grid-Connected Power System by using ISPWM Technique, International Journal of Engineering Trends and Technology (IJETT). V4(5) (2013) 1512-1517 . ISSN:2231-5381
[22] B. Yang, W. Li, Y. Gu, W. Cui, and X. He, Improved Transformerless Inverter with Common-Mode Leakage Current Elimination for a Photovoltaic Grid-Connected Power System, IEEE Trans. on Power Electron., 27(2) (2012) 752–762.
[23] DKE Deutsche Kommission Elektrotechnik Elektronik Information stechnikim DIN und VDE, DIN V VDE V 0126-1-1, (2006).
[24] H. Xiao and S. Xie, Leakage Current Analytical Model and Application in single-Phase Transformerless Photovoltaic Grid-Connected Inverter.IEEE Trans. on Electromagn. Compat., 52(4) (2010) 902–913, Nov 2010
[25] Y. Tang, W. Yao, P. C. Loh, and F. Blaabjerg, Highly Reliable Transformerless Photovoltaic Inverters with Leakage Current and Pulsating Power Elimination, IEEE Trans. on Ind. Electron., 63(2) (2016) 1016–1026.
[26] Ramprasad Panda, R.K. Tripathi, A Symmetrical Hybrid Sine PWM Switching Technique for Full-Bridge Inverters, Proceedings of India International Conference on Power Electronics, (2006).
[27] Ray-Shyang Lai and Khai D. T. Ngo, A PWM Method for Reduction of Switching Loss in a Full-Bridge Inverter, IEEE Transaction on Power Electronics, 10(3) (1995) 326-332.
[28] Yinglai Xia, Raja Ayyanar, Comprehensive Comparison of THD and Common Mode Leakage Current of Bipolar, Unipolar and Hybrid Modulation Schemes for Single Phase Grid Connected Full-Bridge Inverters, (2007).
[29] Mohannad J. Mnati & Alex V. Bossche, Design of A Half-Bridge Circuit for Grid Inverter Application Controlled by Pic 24fj128ga010,. 5th International Conference on Renewable Energy Research and Application, Birmingham IEEE, (2016) 85-89, 20-23 .
[30] Gaurav Sharma, Bhakti Joshi & Ramesh Orugnti, A Double Bootstrap Gate Driving Scheme for HERIC Topology, IEEE , (2018).
[31] SMA Sunny Boy 5.0 - Datasheet, http://www.sma-america-.com, accessed:2020-01-02
[32] Sunways AT5000 - Datasheet, m http://www.technosun.com, accessed:2020-01-04
[33] INGECON SUN IPlay 5TLM - Datasheet, http://www. ingeteam. com, accessed: 2020-01-08.